



Published in final edited form as:

Clin Cancer Res. 2015 May 15; 21(10): 2338–2347. doi:10.1158/1078-0432.CCR-14-3000.

INTRACELLULAR TARGETING OF THE ONCOGENIC MUC1-C PROTEIN WITH A NOVEL GO-203 NANOPARTICLE FORMULATION

Masanori Hasegawa¹, Raj Kumar Sinha², Manoj Kumar², Maroof Alam¹, Li Yin¹, Deepak Raina³, Akriti Kharbanda¹, Govind Panchamoorthy³, Dikshi Gupta², Harpal Singh², Surender Kharbanda³, and Donald Kufe¹

¹Dana-Farber Cancer Institute, Harvard Medical School, Boston, MA 02215

²Center for Biomedical Engineering, Indian Institute of Technology, New Delhi, India

³Genus Oncology, Boston, MA 02118

Abstract

Purpose—The MUC1-C oncoprotein is an intracellular target that is druggable with cell-penetrating peptide inhibitors. However, development of peptidyl drugs for treating cancer has been a challenge because of unfavorable pharmacokinetic parameters and limited cell penetrating capabilities.

Experimental Design—Encapsulation of the MUC1-C inhibitor, GO-203, in novel polymeric nanoparticles (NPs) was studied for effects on intracellular targeting of MUC1-C signaling and function.

Results—Our results show that loading GO-203 into tetrablock polylactic acid (PLA)-polyethylene glycol (PEG)-polypropylene glycol (PPG)-PEG copolymers is achievable and, notably, is enhanced by increasing PEG chain length. Additionally, we found that release of GO-203 from these NPs is controllable over at least 7 days. GO-203/NP treatment of MUC1-C-positive breast and lung cancer cells in vitro was more active with less frequent dosing than that achieved with non-encapsulated GO-203. Moreover, treatment with GO-203/NPs blocked MUC1-C homodimerization, consistent with on-target effects. GO-203/NP treatment was also effective in downregulating TIGAR, disrupting redox balance and inhibiting the self-renewal capacity of cancer cells. Significantly, weekly administration of GO-203/NPs to mice bearing syngeneic or xenograft tumors was associated with regressions that were comparable to those found when dosing on a daily basis with GO-203.

Conclusions—These findings thus define an effective approach for (i) sustained administration of GO-203 in polymeric PLA-(PEG-PPG-PEG) NPs to target MUC1-C in cancer cells and (ii) the potential delivery of other anti-cancer peptide drugs.

Corresponding Authors: Donald Kufe, 450 Brookline Avenue, Dana 830, Boston, Massachusetts, 02215, 617-632-3141 Tel., 617-632-2934 Fax, donald_kufe@dfci.harvard.edu and Harpal Singh, Indian Institute of Technology, Center for Biomedical Engineering, Block 3 Room 297, Hauz Khas, New Delhi, India, 110016, 9810030490 Tel., harpal2000@yahoo.com.

Conflict of Interest: The other authors disclosed no potential conflicts of interest.

Keywords

MUC1-C; GO-203; polymeric nanoparticles; ROS; CSCs

Introduction

The mucin 1 (MUC1) heterodimeric protein is aberrantly overexpressed by breast, lung and other types of carcinomas, and has been recognized as an attractive cancer target (1, 2). Studies on the oncogenic function of MUC1 were advanced by the demonstration that MUC1 consists of two subunits (1). The transmembrane MUC1-C subunit interacts with receptor tyrosine kinases, such as EGFR and HER2, at the cell membrane and contributes to activation of their downstream signaling pathways (3–5). The MUC1-C cytoplasmic domain interacts with the WNT pathway effector, β -catenin, and promotes the activation of WNT target genes in a nuclear complex with TCF7L2/TCF4 (5–7). MUC1-C also interacts with additional transcription factors, including NF- κ B and STAT3, in the regulation of gene expression (5). The involvement of MUC1-C with effectors that have been linked to transformation (5) and the demonstration that MUC1-C drives self-renewal of cancer cells (8–10) have provided support for the development of agents that block MUC1-C function. In this respect, the MUC1-C cytoplasmic domain contains a CQC motif that is necessary and sufficient for MUC1-C homodimerization (5). Additionally, mutation of the CQC motif to AQA blocks the capacity of MUC1-C to interact with diverse effectors and function as an oncoprotein (11). Based on these observations, a novel class of cell-penetrating peptides was developed to bind to the CQC motif and thereby block MUC1-C homodimerization and signaling (12, 13). The MUC1-C targeted peptides induce death of MUC1-expressing cancer cells in vitro and inhibit growth of established tumor xenografts in mice (12, 14, 15). As shown for other small therapeutic peptides (16), the MUC1-C inhibitor peptides exhibited short circulating half-lives and thus required daily administration for sustained inhibition of tumor growth in mouse models (12, 14, 15). These findings provided the basis for Phase I evaluation of the lead MUC1-C inhibitor peptide, designated GO-203, in patients with refractory solid tumors.

Cell-penetrating anti-cancer peptides are emerging as promising agents to target intracellular proteins that are otherwise undruggable with small molecule inhibitors. For example, peptide drugs are under preclinical development to target proteins devoid of ATP binding pockets, such as survivin (17), β -catenin (18), HDM2 (19), STAT3 (20) and E2F (21), and others. However and as noted above, adequate delivery of peptides to tumors can be challenging because of unfavorable pharmacokinetic parameters (16). Administration of peptide drugs can also be limited by their proteolytic degradation or the induction of immune responses. Accordingly, improved delivery systems are needed, at least in part, for the successful development of anti-cancer peptides. Nanoparticles (NPs) have been employed to improve the pharmacokinetic properties and therapeutic indices of small molecule anti-cancer agents, such as doxorubicin and paclitaxel (22). In this way, NPs have the capacity to sustain drug exposure in the tumor microenvironment by the enhanced permeation and retention (EPR) effect (23). In addition, NPs can be modified with ligands that bind to targets selectively expressed on the surface of tumor cells (24). Among different

classes of NPs, polylactic acid (PLA)-polyethylene glycol (PEG) block copolymer NPs are non-toxic and biodegradable (24). In addition, the polymeric PLA-PEG NPs have been administered clinically for the delivery of small molecule anti-cancer agents (24). By contrast and to our knowledge, polymeric NPs have not been explored for the delivery of anti-cancer peptides, other than in a recent preclinical study (25). In this regard, anti-cancer peptides have been incorporated into cationic liposomes (26), perfluorocarbon nanoemulsion vehicles (27), cyclodextrin polymerized NPs (28), and liposome-protamine-heparin NPs (29). However, unlike polymeric NPs, these NP formulations have evidently not been advanced for clinical applications.

The present studies have investigated the encapsulation of GO-203 into polymeric tetrablock NPs as a delivery system to target the oncogenic MUC1-C protein in cancer cells. The results demonstrate that the delivery of GO-203 in NPs is an effective approach for inhibiting intracellular MUC1-C homodimerization and function. Our findings thus provide support for the further development of GO-203/NPs as a therapeutic for the treatment of MUC1-C-expressing malignancies.

Materials and Methods

Preparation of GO-203-loaded NPs

Poly(lactic acid (PLA)-poly(ethylene glycol (PEG)-poly(propylene glycol (PPG)-PEG) tetrablock copolymers were synthesized as described (25). The NPs were loaded with GO-203 (15) and filtered through an Amikon 10-kDa ultrafilter (Millipore). The filtrate was collected and analyzed for free GO-203 peptide using a Micro-BCA Kit (Pierce Chemicals). Encapsulation efficiency (EE), particle size and zeta potential were determined as described (25).

Assessment of GO-203 release from NPs

The *in vitro* release kinetics of GO-203 from NPs were determined by the ultrafiltration method as described (25).

Cell culture

ZR-75-1 breast cancer, and H1975 and H460 lung cancer cells (ATCC) were grown in RPMI1640 media supplemented with 10% heat-inactivated fetal bovine serum (HI-FBS), 100 µg/ml streptomycin and 100 units/ml penicillin. MCF-7 and MDA-MB-468 breast cancer cells, and HCT116 colon cancer cells (ATCC) were cultured in DMEM media supplemented with HI-FBS and antibiotics. BT-20 breast cancer cells (ATCC) were grown in EMEM media containing HI-FBS and antibiotics. Cells were treated with the MUC1-C inhibitor GO-203 (15) encapsulated in PLA-(PEG-PPG-PEG)^{12.5K} NPs (GO-203/NPs), the control peptide CP-2 (15) encapsulated in PLA-(PEG-PPG-PEG)^{12.5K}NPs (CP-2/NPs) or unloaded, empty NPs.

Analysis of cell viability

Cells were seeded on 96-well plates in 100 µl growth medium at a density of 1000–2000 cells per well. After 24 h, the cells were exposed to one treatment of NPs on day 0 or two

treatments of NPs on day 0 and 3. Cell viability was determined in triplicates using the Alamar blue assay on day 3 or 7. Statistical significance between treatment groups was assessed using the Student's t-test.

Immunoblot analysis

Cell lysates were prepared as described (15). Soluble proteins were analyzed by immunoblotting with anti-MUC1-C (30), anti-TIGAR (Abcam), anti-phospho-p38, anti-p38 (Cell Signaling Technologies), or anti- β -actin (Sigma) as described (15). Immune complexes were detected with horseradish peroxidase-conjugated secondary antibodies and enhanced chemiluminescence (PerkinElmer).

Measurement of NADPH and GSH levels

Intracellular NADPH and GSH levels were measured using the Enzychrom NADP/NADPH Assay Kit (BioAssay Systems) and the Bioxytech GSH-400 kit (OXIS International), respectively.

Colony formation assays

Cells were seeded in 6-well plates for 24 h and then left untreated or treated with NPs. After 10–20 d, the cells were washed and stained with 0.5% crystal violet in 25% methanol. Colonies >30 cells were counted in triplicate wells.

Tumor spheres

Cells were harvested with gentle trypsinization, washed and resuspended in MammoCult™ Human Medium (Stem Cell Technologies). Single cells were confirmed under a microscope, counted, seeded in 6-well ultralow attachment culture plates (Corning CoStar) and cultured for 5 days. Tumor spheres of 100 μ m were visualized and scored using a Nikon inverted TE2000 microscope. Sphere forming efficiency (SFE) was calculated by dividing the number of tumor spheres by the number of suspended cells.

Assessment of anti-tumor activity

Mouse Ehrlich breast tumor cells were injected subcutaneously in the hind limb of syngeneic Balb/c mice (17–22 gms). Mice bearing tumors (~40 mm³) were divided into groups of 10 mice each and treated intraperitoneally (IP) (i) each day with vehicle control or 15 mg/kg GO-203 for 21 days, or (ii) once each week with 10, 15 or 20 mg/kg GO-203/NPs for 3 weeks. Four- to 6-week old Balb/c nu/nu mice were injected subcutaneously with 5×10^6 ZR-75-1 cells in the flank. Mice with established ZR-75-1 tumors (90–120 mm³) were randomized into groups of 6 mice each and treated IP (i) each day with vehicle control or 18 mg/kg GO-203 for 21 days, or (ii) once each week with vehicle control or 20 mg/kg GO-203/NPs for 3 weeks. Tumors were measured every other day with calipers, and tumor volumes were calculated using the formula $(A \times B^2) \times 0.5$, where A and B are the longest and shortest tumor diameters, respectively. Statistical analysis of tumor volumes was performed by one-way ANOVA and the Dunnett test using Origin 8.0 (Origin Lab, Northampton, MA).

Results

Encapsulation of GO-203 into NPs

Polymeric NPs are being increasingly used for the delivery of small molecules (24, 31, 32); however, the experience with encapsulation of peptidyl drugs into NPs is presently limited and will probably be dictated by the characteristics of the specific peptides under investigation. The present studies have focused on encapsulation of the MUC1-C inhibitor GO-203 peptide into tetrablock polymeric NPs comprised of copolymers of PLA modified with polyethylene glycol (PEG)-polypropylene glycol (PPG) (PEG-PPG-PEG)^{12.5K} (25). GO-203 is an all D-amino acid peptide that consists of a poly-R transduction domain linked to a CQCRRKN motif that binds to the MUC1-C cytoplasmic tail and blocks MUC1-C homodimerization (13, 15) (Fig. 1A). Encapsulation of GO-203 into the core of the NPs was increased by PEG modification (Supplemental Table S1). Thus, the encapsulation efficiency of GO-203 in PLA-PEG⁴⁰⁰⁰NPs was higher than that obtained with PLA-PEG⁶⁰⁰ NPs (Supplemental Table S1). We also found that increases in PEG chain length improved the GO-203 encapsulation efficiency (Supplemental Table S1). We next studied the kinetics of GO-203 release from PLA-(PEG-PPG-PEG)^{12.5K}NPs. At pH 7.4, the percentage release/day of the encapsulated GO-203 decreased from ~15% on day 1 to ~4% on day 5, and then slowly declined over the next 55 days (Fig. 1B). In terms of cumulative release, over 50% of the encapsulated GO-203 was released by day 7 (Fig. 1C). These findings collectively provided support for prolonged kinetics of GO-203 release at physiologic pH. Accordingly, subsequent studies were performed with GO-203 encapsulated in PLA-(PEG-PPG-PEG)^{12.5K}NPs (GO-203/NPs).

Treatment with GO-203/NPs decreases survival of breast cancer cells

GO-203 is effective in inducing death of MUC1-expressing breast and other types of cancer cells (3, 15, 33, 34). To determine whether encapsulated GO-203 is also effective in inhibiting cell viability, we first treated ZR-75-1 breast cancer cells with 7.5 μ M GO-203/NPs. In these studies, a single exposure to GO-203/NPs on day 0 was associated with loss of survival as detected on day 3 (Fig. 2A, left). By contrast, treatment with empty NPs had little if any effect on cell viability (Fig. 2A, left). Similar results were obtained when MDA-MB-468 breast cancer cells were treated once with 7.5 μ M GO-203/NPs or empty NPs and analyzed on day 3 (Fig. 2A, right), confirming that GO-203 is active when delivered from NPs. Moreover, treatment once with 7.5 μ M GO-203/NPs was more effective than exposure to 2.5 μ M GO-203 (non-encapsulated) each day for 3 days (Fig. 2A, right). Based on these results, we explored the effects of GO-203/NPs and non-encapsulated GO-203 at different doses and schedules. In this way, we compared treatment of ZR-75-1 cells with 2.5 μ M GO-203/NPs or 2.5 μ M GO-203 on days 0 and 3 (Fig. 2B, left). Analysis of the cells on day 7 showed that the GO-203/NPs are more effective than GO-203 (Fig. 2B, left). Treatment of MDA-MB-468 cells with 5 μ M GO-203/NPs or GO-203 on days 0 and 3 further demonstrated that loss of survival was greater with GO-203/NPs, as compared to GO-203, treatment (Fig. 2B, right).

To extend this analysis, BT-20 breast cancer cells were treated on day 0 with 7.5 or 10 μ M GO-203/NPs or equal amounts of empty NPs (Fig. 2C). As an additional control, cells were

treated with NPs containing a peptide (CP-2) that consists of poly-R linked to AQARRKN (Fig. 1A), which is inactive in binding to the MUC1-C cytoplasmic domain and ineffective in killing MUC1-expressing cells (3, 15, 33, 34). As analyzed on day 3, treatment with GO-203/NPs was associated with a significant loss of survival as compared to that obtained with empty NPs, which had little if any effect (data not shown) or with CP-2/NPs (Fig. 2C). Moreover, treatment with 2.5 or 3.3 μM unencapsulated GO-203 on days 0, 1 and 2 was clearly less effective than exposure to the same amounts of GO-203 in NPs that was administered once (Fig. 2C). In contrast to these results, a similar study performed on MUC1-negative HCT116 cells demonstrated no significant difference in survival upon treatment with GO-203/NPs, CP-2/NPs or unencapsulated GO-203 (Fig. 2D). These findings indicated that GO-203-induced loss of cell viability is more effective when delivered in NPs and is selective for MUC1-positive cells.

GO-203/NPs disrupt MUC1-C homodimerization and disrupt redox balance in breast cancer cells

Targeting MUC1-C with unencapsulated GO-203 induces death of carcinoma cells by blocking MUC1-C homodimerization and thereby disrupting redox balance (13, 15). To determine whether delivery of GO-203 in NPs induces similar effects, we first treated ZR-75-1 cells with GO-203/NPs and monitored effects on MUC1-C homodimerization. As found with non-encapsulated GO-203 (13), treatment with GO-203/NPs was associated with inhibition of MUC1-C homodimer formation (Fig. 3A), indicating that delivery of GO-203 in NPs to these carcinoma cells results in MUC1-C targeting. MUC1-C promotes expression of the p53-inducible regulator of glycolysis and apoptosis (TIGAR) (35), which shunts glucose-6-phosphate into the pentose phosphate pathway (PPP) (36). Consistent with targeting MUC1-C, we found that treatment of ZR-75-1 cells with GO-203/NPs is associated with suppression of TIGAR levels (Fig. 3B). Moreover, addition of the antioxidant NAC blocked GO-203/NP-induced TIGAR suppression (Fig. 3B), in concert with a ROS-mediated mechanism. TIGAR promotes the production of NADPH and GSH by the PPP (36). In this way, targeting MUC1-C with GO-203/NPs was also associated with marked decreases in NADPH (Fig. 3C, left) and GSH (Fig. 3C, right) levels. Moreover, and consistent with these results, we found that treatment with GO-203/NPs, but not CP-2/NPs, results in induction of phospho-p38 (Fig. 3D), which is activated in response to disruption of redox balance (37).

GO-203/NPs are effective against NSCLC cells

NSCLC cells are also sensitive to GO-203 treatment (15). Accordingly, we asked if NSCLC cells respond similarly to GO-203/NPs. Indeed, GO-203/NP treatment of H1975 NSCLC cells, which harbor the EGFR(L858R/T790M) mutations, was associated with loss of viability (Fig. 4A, left). Other studies performed with H460/KRAS(Q61H) NSCLC cells further demonstrated that GO-203/NPs are active in the setting of mutant KRAS expression (Fig. 4A, right). By contrast, exposure of H1975 and H460 NSCLC cells to empty NPs was associated with substantially lower levels of cell death that were not significantly different from those obtained for ZR-75-1 and MDA-MB-468 breast cancer cells (Fig. 2A, left and right). As shown for breast cancer cells, we also found that treatment of H1975 cells with GO-203/NPs is associated with disruption of MUC1-C homodimers (Fig. 4B, left).

Moreover, GO-203 treatment resulted in downregulation of TIGAR (Fig. 4B, right) and decreases in NADPH (Fig. 4C, left) and GSH (Fig. 4C, right) levels. Treatment of H1975 cells with GO-203/NPs was also associated with activation of p-p38 (Fig. 4D), confirming that delivery of GO-203 in NPs is effective in disrupting redox balance.

GO-203/NPs inhibit breast and lung cancer cell self-renewal

Disruption of redox balance inhibits the capacity of cancer cells to undergo self-renewal (38). Accordingly, we first investigated the effects of GO-203/NPs on clonogenic survival of ZR-75-1 cells. Treatment with the GO-203/NPs, but not the empty NPs, was highly effective in inhibiting colony formation (Fig. 5A, left). Similar results were obtained with GO-203/NP treatment of MDA-MB-468 (Fig. 5A, middle) and MCF-7 (Fig. 5A, right) cells, indicating that GO-203/NP exposure is sufficient to inhibit clonogenic survival of breast cancer cells. The formation of spheres under non-adherent conditions and in the absence of serum selects for the growth of self-renewing cancer stem-like cells (CSCs) that survive anoikis (39, 40). Therefore, to determine if the GO-203/NPs are active against self-renewing populations, MDA-MB-468 cells were treated with GO-203/NPs or CP-2/NPs for 48 h and then grown in mammosphere medium in the absence of NPs. As expected from previous studies (9), the control MDA-MB-468 cells formed mammospheres (Fig. 5B). Moreover, treatment with GO-203/NPs, but not CP-2/NPs, was highly effective in inhibiting mammosphere formation and decreasing sphere-forming efficiency (SFE) (Fig. 5B). GO-203/NPs also inhibited MCF-7 mammosphere formation (Fig. 5C), supporting the activity of GO-203/NPs against self-renewing breast cancer cells.

In investigating the effects of GO-203/NPs against clonogenic NSCLC cell populations, we found that GO-203/NPs completely inhibited H1975 (Supplemental Fig. S1A) and H460 (Supplemental Fig. S1B) colony formation. Moreover, GO-203/NP treatment blocked growth of H1975 (Supplemental Fig. S1C) and H460 (Supplemental Fig. S1D) cells as spheres, indicating that encapsulation of GO-203 in NPs is effective in inhibiting self-renewal of NSCLC cells.

GO-203/NPs inhibit tumor growth

To investigate whether GO-203/NPs are effective in inhibiting growth of human tumor xenografts in nude mice, we first performed studies in Balb/c mice bearing established subcutaneous syngeneic Muc1-positive Ehrlich breast tumors. In this model and consistent with previous studies of human tumor xenograft models (15), treatment with non-encapsulated GO-203 was associated with inhibition of Ehrlich tumor growth (Fig. 6A). Based on the kinetics of GO-203 release from the NPs over 7 days (Fig. 1C), we treated the Ehrlich tumor bearing mice IP once a week for 3 weeks with doses of 10, 15 or 20 mg/kg GO-203/NPs (Fig. 6B). As compared to the control mice, treatment with 10 mg/kg GO-203/NPs was associated with partial slowing of Ehrlich tumor growth (Fig. 6B). By contrast, IP dosing of 15 and 20 mg/kg GO-203/NPs resulted in complete inhibition of Ehrlich tumor growth, supporting a dose-response effect (Fig. 6B). In previous studies of nude mice bearing subcutaneous NSCLC xenografts, treatment with non-encapsulated 30 mg/kg GO-203 IP daily for 21 days was associated with complete regressions (15). In the present work, IP administration of GO-203 each day at a dose of 18 mg/kg was also

effective in the treatment of ZR-75-1 xenografts (Fig. 6C). Notable findings in these experiments were that treatment with GO-203 on a weekly or twice-weekly schedule had little if any effect on ZR-75-1 tumor growth, indicating that frequent (daily) dosing is necessary for activity (data not shown). By comparison, weekly treatment of ZR-75-1 xenografts with GO-203/NPs at a dose of 20 mg/kg was highly effective in inducing tumor regressions (Fig. 6D). Significantly, there was no overt evidence of toxicity, such as weight loss, associated with GO-203/NP administration. These findings thus support the notion that delivery of GO-203 in NPs requires less frequent administration and lower total doses than that needed for equivalent anti-tumor activity when treating with non-encapsulated GO-203.

Discussion

The oncogenic MUC1-C protein is aberrantly expressed in carcinomas of the breast, lung and other epithelia (1, 5). Additionally, recent evidence has supported a role for MUC1-C in promoting the epithelial-mesenchymal transition (EMT) and other characteristics of CSCs (8, 9). These findings have collectively provided the rationale for developing therapeutic approaches that target MUC1-C function. The present studies have identified a novel strategy for targeting MUC1-C in carcinoma cells by intracellular delivery of the peptidyl MUC1-C inhibitor, GO-203, in polymeric NPs. Cell-penetrating peptides have emerged as promising therapeutics because of their potential for targeting intracellular proteins that lack hydrophobic pockets and thereby are often undruggable with small molecules. Moreover, peptidyl drugs have the potential for inhibiting intracellular proteins with greater specificity and less off-target toxicity than small molecules (41, 42). Nonetheless, the development of peptidyl drugs can be hampered by poor pharmacologic properties, such as short circulating half-lives, that require frequent administration (16). Therapeutic peptides can also be limited by extracellular degradation and inefficient cell penetrating capabilities. Accordingly, the present work first investigated whether GO-203 could indeed be loaded into NPs.

There is presently limited information about the optimal conditions for encapsulating peptides into polymeric NPs and the copolymers used will likely vary depending on the peptidyl drug itself. The approach we used in the present work was based upon a recent experience in which we encapsulated the anticancer peptide NuBCP-9 into tetrablock PLA-(PEG-PPG-PEG)^{12.5K} copolymers (25). The PLA-PEG copolymer is a bilayer structure with a PLA hydrophobic core and a PEG hydrophilic shell interacting with the aqueous medium. The importance of the tetrablock structure is that conjugation of PEG-PPG-PEG with PLA extends the hydrophobic core and thereby has the capacity for increasing peptide uptake and sustaining its release (25). The PLA-PEG-PPG-PEG formulation was thus selected based on the findings demonstrating that (i) peptide encapsulation is greater than that obtained with PLA, and (ii) peptide release is more sustained compared to that found for the PLA-PEG NPs (25). Indeed, as compared to PLA-based NPs, we found that loading of GO-203 is increased with PLA-PEG-PPG-PEG NPs. We also found that approximately 50% of the GO-203 encapsulated into PLA-PEG-PPG-PEG NPs is released over 7 days at physiologic pH, which appeared to be favorable kinetics when considering that an objective of delivering GO-203 in NPs to cancer cells would be prolonged intracellular exposure of endogenous MUC1-C to this agent.

Non-encapsulated GO-203 is effective in inducing death of MUC1-positive carcinoma cells in vitro when low μM concentrations are added each day to the medium over 4–6 days (15). Importantly, the present studies show that encapsulation of GO-203 in NPs is also effective in killing breast and lung cancer cells, indicating that loading of GO-203 into NPs is not associated with loss of activity. Indeed, we found that treatment with the GO-203/NPs is even more effective than that obtained with non-encapsulated GO-203 at equivalent doses. Moreover, delivery of GO-203 in NPs required less frequent dosing than non-encapsulated GO-203. As one of several examples in support of this contention, a single exposure of cancer cells to 7.5 μM GO-203/NPs was far more active in inducing cell death than treatment with 2.5 μM GO-203 each day for 3 days (Fig. 3E). GO-203 blocks MUC1-C homodimerization by targeting the MUC1-C CQC motif (13). As confirmation that GO-203 functions similarly when loaded into NPs, we found that treatment with GO-203/NPs also inhibits the formation of MUC1-C homodimers, supporting similar effects on MUC1-C targeting. Studies in malignant hematopoietic cells that express MUC1-C have demonstrated that GO-203 treatment downregulates TIGAR and thereby induces redox imbalance by decreasing NADPH and GSH levels (35, 43). The present results extend these observations to breast and lung cancer cells by demonstrating that treatment with GO-203 and GO-203/NPs also suppresses TIGAR expression in association with decreases in NADPH and GSH. The GO-203-induced signals responsible for TIGAR downregulation in carcinoma cells will require further study; however, these observations further indicate that GO-203/NPs induce loss of self-renewal in association with disruption of redox balance. In concert with this notion, GO-203/NPs were highly effective in inhibiting clonogenic survival and tumor sphere formation of breast and lung cancer cells. Taken together, these findings indicate that encapsulation of GO-203 in NPs is an effective approach for the delivery of GO-203 to cancer cells and that GO-203/NPs function similarly to GO-203 in terms of inhibiting MUC1-C homodimerization and downstream signaling pathways.

NP delivery systems for cancer treatment with small molecules have been developed to improve pharmacokinetic properties and increase the therapeutic index (22). In addition and through the EPR effect, NP delivery can sustain drug exposure in the tumor microenvironment (22, 23). However, the experience with NP delivery of anti-cancer peptides remains limited. The present results demonstrate that loading of GO-203 into polymeric NPs markedly improves the delivery of GO-203 as an anti-cancer agent in vivo. In this way, the anti-cancer activity of non-encapsulated GO-203 requires daily administration to sustain tumor exposure, consistent with a short circulating half-life in mice (15). By comparison, administration of GO-203/NPs once weekly was sufficient to confer a similar level of anti-tumor activity to that achieved with daily delivery of GO-203. The marked enhancement of anti-tumor activity found with GO-203/NPs could be attributed in part to the EPR effect. In addition, uptake of GO-203/NPs by tumor cells and the sustained release of GO-203, as observed over 7 days at physiologic pH, likely also contribute to more prolonged effects on intracellular targeting of MUC1-C function. These findings with GO-203/NPs are in concert with the recent demonstration that in vivo anti-cancer activity of the NuBCP-9 peptide is markedly increased by delivery in polymeric NPs, suggesting that this NP approach may be broadly applicable for other peptides that target intracellular effectors. Polymeric NPs have been widely studied and certain formulations have been

found to be nontoxic and biodegradable (24, 31). For example, with degradation of PLA from the PLA-PEG-PPG-PEG NPs used in the present work, the resulting PEG-PPG-PEG triblock (~12.5 kDa) is a nontoxic polymer that is an FDA approved biomaterial for clinical use (44). With regard to polymeric NPs already in the clinic, Genexol-PM is a paclitaxel loaded PLA-PEG-based NP that is undergoing Phase II evaluation for the treatment of metastatic cancers (24, 32). Moreover, BIND Biosciences is evaluating docetaxel-encapsulated biodegradable polymeric NPs for the treatment of patients with solid tumors (24). These ongoing clinical trials with polymeric NPs and the present results thus provide support for the further development of GO-203/NPs as a potential therapeutic agent. In this respect, a Phase I trial of non-encapsulated GO-203 administered on a daily basis has been completed and a maximum tolerated dose has been defined for Phase II trials. Our findings here thus lend credence to the notion that GO-203 could be delivered in additional Phase II studies on a less frequent schedule and at potentially lower total doses by encapsulation in polymeric NPs.

Supplementary Material

Refer to Web version on PubMed Central for supplementary material.

Acknowledgments

Financial Support: Research supported in this publication was supported by the National Cancer Institute of the National Institutes of Health under award numbers CA166480 and CA97098, by the Lung Cancer Research Foundation and by the Department of Science and Technology, Government of India.

D.K. holds equity in Genus Oncology and is a consultant to the company.

Abbreviations

MUC1	mucin 1
MUC1-C	MUC1 C-terminal subunit
NPs	nanoparticles
PLA	polylactic acid
PEG	polyethylene glycol
PPG	polypropylene glycol
TIGAR	p53-inducible regulator of glycolysis and apoptosis
ROS	reactive oxygen species
EPR	enhanced permeation and retention
CSCs	cancer stem-like cells
SFE	sphere forming efficiency
EMT	epithelial-mesenchymal transition

References

1. Kufe D. Mucins in cancer: function, prognosis and therapy. *Nature Reviews Cancer*. 2009; 9:874–885.
2. Cheever MA, Allison JP, Ferris AS, Finn OJ, Hastings BM, Hecht TT, et al. The prioritization of cancer antigens: a national cancer institute pilot project for the acceleration of translational research. *Clin Cancer Res*. 2009; 15:5323–5337. [PubMed: 19723653]
3. Raina D, Uchida Y, Kharbanda A, Rajabi H, Panchamoorthy G, Jin C, et al. Targeting the MUC1-C oncoprotein downregulates HER2 activation and abrogates trastuzumab resistance in breast cancer cells. *Oncogene*. 2013 advance online publication 5 August.
4. Kharbanda A, Rajabi H, Jin C, Tchaicha J, Kikuchi E, Wong K, et al. Targeting the oncogenic MUC1-C protein inhibits mutant EGFR-mediated signaling and survival in non-small cell lung cancer cells. *Clin Cancer Res*. 2014; 20:5423–5434. [PubMed: 25189483]
5. Kufe D. MUC1-C oncoprotein as a target in breast cancer: activation of signaling pathways and therapeutic approaches. *Oncogene*. 2013; 32:1073–1081. [PubMed: 22580612]
6. Huang L, Chen D, Liu D, Yin L, Kharbanda S, Kufe D. MUC1 oncoprotein blocks GSK3 β -mediated phosphorylation and degradation of β -catenin. *Cancer Res*. 2005; 65:10413–10422. [PubMed: 16288032]
7. Rajabi H, Ahmad R, Jin C, Kosugi M, Alam M, Joshi M, et al. MUC1-C oncoprotein induces TCF7L2 activation and promotes cyclin D1 expression in human breast cancer cells. *J Biol Chem*. 2012; 287:10703–10713. [PubMed: 22318732]
8. Rajabi H, Alam M, Takahashi H, Kharbanda A, Guha M, Ahmad R, et al. MUC1-C oncoprotein activates the ZEB1/miR-200c regulatory loop and epithelial-mesenchymal transition. *Oncogene*. 2013; 33:1680–1689. [PubMed: 23584475]
9. Alam M, Rajabi H, Ahmad R, Jin C, Kufe D. Targeting the MUC1-C oncoprotein inhibits self-renewal capacity of breast cancer cells. *Oncotarget*. 2014; 5:2622–2634. [PubMed: 24770886]
10. Kharbanda A, Rajabi H, Jin C, Alam M, Wong K, Kufe D. MUC1-C confers EMT and KRAS independence in mutant KRAS lung cancer cells. *Oncotarget*. 2014; 5:8893–8905. [PubMed: 25245423]
11. Kufe D. Functional targeting of the MUC1 oncogene in human cancers. *Cancer Biol Ther*. 2009; 8:1201–1207.
12. Raina D, Ahmad R, Joshi M, Yin L, Wu Z, Kawano T, et al. Direct targeting of the MUC1 oncoprotein blocks survival and tumorigenicity of human breast carcinoma cells. *Cancer Res*. 2009; 69:5133–5141. [PubMed: 19491255]
13. Raina D, Ahmad R, Rajabi H, Panchamoorthy G, Kharbanda S, Kufe D. Targeting cysteine-mediated dimerization of the MUC1-C oncoprotein in human cancer cells. *Int J Oncol*. 2012; 40:1643–1649. [PubMed: 22200620]
14. Joshi MD, Ahmad R, Raina D, Rajabi H, Bublely G, Kharbanda S, et al. MUC1 oncoprotein is a druggable target in human prostate cancer cells. *Mol Cancer Ther*. 2009; 8:3056–3065. [PubMed: 19887552]
15. Raina D, Kosugi M, Ahmad R, Panchamoorthy G, Rajabi H, Alam M, et al. Dependence on the MUC1-C oncoprotein in non-small cell lung cancer cells. *Mol Cancer Therapeutics*. 2011; 10:806–816.
16. Talmadge JE. Pharmacodynamic aspects of peptide administration biological response modifiers. *Adv Drug Deliv Rev*. 1998; 33:241–252. [PubMed: 10837664]
17. Plescia J, Salz W, Xia F, Pennati M, Zaffaroni N, Daidone MG, et al. Rational design of shepherdin, a novel anticancer agent. *Cancer Cell*. 2005; 7:457–468. [PubMed: 15894266]
18. Grossmann TN, Yeh JT, Bowman BR, Chu Q, Moellering RE, Verdine GL. Inhibition of oncogenic Wnt signaling through direct targeting of beta-catenin. *Proc Natl Acad Sci U S A*. 2012; 109:17942–17947. [PubMed: 23071338]
19. Sarafraz-Yazdi E, Bowne WB, Adler V, Sookraj KA, Wu V, Shteyler V, et al. Anticancer peptide PNC-27 adopts an HDM-2-binding conformation and kills cancer cells by binding to HDM-2 in their membranes. *Proc Natl Acad Sci U S A*. 2010; 107:1918–1923. [PubMed: 20080680]

20. Kim D, Lee IH, Kim S, Choi M, Kim H, Ahn S, et al. A Specific STAT3-Binding Peptide Exerts Antiproliferative Effects and Antitumor Activity by Inhibiting STAT3 Phosphorylation and Signaling. *Cancer Res.* 2014; 74:1–8.
21. Xie X, Bansal N, Shaik T, Kerrigan J, Minko T, Garbuzenko O, et al. A novel peptide that inhibits E2F transcription and regresses prostate tumor xenografts. *Oncotarget.* 2014; 5:901–907. [PubMed: 24658650]
22. Kratz F, Warnecke A. Finding the optimal balance: challenges of improving conventional cancer chemotherapy using suitable combinations with nano-sized drug delivery systems. *J Control Release.* 2012; 164:221–235. [PubMed: 22705248]
23. Manzoor AA, Lindner LH, Landon CD, Park JY, Simnick AJ, Dreher MR, et al. Overcoming limitations in nanoparticle drug delivery: triggered, intravascular release to improve drug penetration into tumors. *Cancer Res.* 2012; 72:5566–5575. [PubMed: 22952218]
24. Kamaly N, Xiao Z, Valencia PM, Radovic-Moreno AF, Farokhzad OC. Targeted polymeric therapeutic nanoparticles: design, development and clinical translation. *Chem Soc Rev.* 2012; 41:2971–3010. [PubMed: 22388185]
25. Kumar M, Gupta D, Singh G, Sharma S, Bhatt M, Prashant CK, et al. Novel polymeric nanoparticles for intracellular delivery of peptide cargos: antitumor efficacy of the BCL-2 conversion peptide NuBCP-9. *Cancer Res.* 2014; 74:1–11.
26. Ko YT, Falcao C, Torchilin VP. Cationic liposomes loaded with proapoptotic peptide D-(KLAKLAK)(2) and Bcl-2 antisense oligodeoxynucleotide G3139 for enhanced anticancer therapy. *Mol Pharm.* 2009; 6:971–977. [PubMed: 19317442]
27. Soman NR, Baldwin SL, Hu G, Marsh JN, Lanza GM, Heuser J, et al. Molecularly targeted nanocarriers deliver the cytolytic peptide melittin specifically to tumor cells in mice, reducing cell growth. *J Clin Invest.* 2009; 119:2830–2842. [PubMed: 19726870]
28. Schluep T, Gunawan P, Ma L, Jensen GS, Düringer J, Hinton S, et al. Polymeric tubulysin-peptide nanoparticles with potent antitumor activity. *Clin Cancer Res.* 2009; 15:181–189. [PubMed: 19118045]
29. Kim SK, Huang L. Nanoparticle delivery of a peptide targeting EGFR signaling. *J Control Release.* 2012; 157:279–286. [PubMed: 21871507]
30. Panchamoorthy G, Rehan H, Kharbanda A, Ahmad R, Kufe D. A monoclonal antibody against the oncogenic mucin 1 cytoplasmic domain. *Hybridoma.* 2011; 30:531–535. [PubMed: 22149278]
31. Xiao RZ, Zeng ZW, Zhou GL, Wang JJ, Li FZ, Wang AM. Recent advances in PEG-PLA block copolymer nanoparticles. *Int J Nanomedicine.* 2010; 5:1057–1065. [PubMed: 21170353]
32. Kim TY, Kim DW, Chung JY, Shin SG, Kim SC, Heo DS, et al. Phase I and pharmacokinetic study of Genexol-PM, a cremophor-free, polymeric micelle-formulated paclitaxel, in patients with advanced malignancies. *Clin Cancer Res.* 2004; 10:3708–3716. [PubMed: 15173077]
33. Uchida Y, Raina D, Kharbanda S, Kufe D. Inhibition of the MUC1-C oncoprotein is synergistic with cytotoxic agents in treatment of breast cancer cells. *Cancer Biol Ther.* 2013; 14:127–134. [PubMed: 23114713]
34. Kharbanda A, Rajabi H, Jin C, Raina D, Kufe D. MUC1-C oncoprotein induces tamoxifen resistance in human breast cancer. *Mol Cancer Res.* 2013; 11:714–723. [PubMed: 23538857]
35. Yin L, Kosugi M, Kufe D. Inhibition of the MUC1-C oncoprotein induces multiple myeloma cell death by downregulating TIGAR expression and depleting NADPH. *Blood.* 2012; 119:810–816. [PubMed: 22117045]
36. Bensaad K, Tsuruta A, Selak MA, Vidal MN, Nakano K, Bartrons R, et al. TIGAR, a p53-inducible regulator of glycolysis and apoptosis. *Cell.* 2006; 126:107–120. [PubMed: 16839880]
37. Muller M. Cellular senescence: molecular mechanisms, in vivo significance, and redox considerations. *Antioxid Redox Signal.* 2009; 11:59–98. [PubMed: 18976161]
38. Shi X, Zhang Y, Zheng J, Pan J. Reactive oxygen species in cancer stem cells. *Antioxid Redox Signal.* 2012; 16:1215–1228. [PubMed: 22316005]
39. Dontu G, Abdallah WM, Foley JM, Jackson KW, Clarke MF, Kawamura MJ, et al. In vitro propagation and transcriptional profiling of human mammary stem/progenitor cells. *Genes Dev.* 2003; 17:1253–1270. [PubMed: 12756227]

40. Liao MJ, Zhang CC, Zhou B, Zimonjic DB, Mani SA, Kaba M, et al. Enrichment of a population of mammary gland cells that form mammospheres and have in vivo repopulating activity. *Cancer Res.* 2007; 67:8131–8138. [PubMed: 17804725]
41. Bidwell GL 3rd, Raucher D. Therapeutic peptides for cancer therapy. Part I - peptide inhibitors of signal transduction cascades. *Expert Opin Drug Deliv.* 2009; 6:1033–1047. [PubMed: 19637980]
42. Raucher D, Moktan S, Massodi I, Bidwell GL 3rd. Therapeutic peptides for cancer therapy. Part II - cell cycle inhibitory peptides and apoptosis-inducing peptides. *Expert Opin Drug Deliv.* 2009; 6:1049–1064. [PubMed: 19743895]
43. Yin L, Kufe T, Avigan D, Kufe D. Targeting the MUC1-C oncoprotein is synergistic with bortezomib in downregulating TIGAR and inducing ROS-mediated multiple myeloma cell death. *Blood.* 2014; 123:2997–3006. [PubMed: 24632713]
44. Lee SY, Lee Y, Chae SU, Park TG, Ahn C. Blends of oppositely charged PEG-PPG-PEG copolymers displaying improved physical thermogelling properties. *Macromol Chem Phy.* 2010; 211:692–697.

Statement of Translational Relevance

Intracellular cancer targets devoid of a kinase domain are often undruggable with small molecule inhibitors. In this context, anti-cancer peptides, such as GO-203, which inhibits the MUC1-C oncoprotein, are an alternative class of agents for targeting intracellular proteins. The development of anti-cancer peptide drugs, however, has been limited by their immunogenicity, short circulating half-life and poor cell penetration. The present work has studied the incorporation of GO-203 into nanoparticles comprised of a novel PLA-PEG-PPG-PEG tetrablock copolymer. Our results demonstrate that these nanoparticles are highly effective for the encapsulation and then release of GO-203 over sustained periods of time. Our findings further demonstrate that this nanoparticle-based approach for intracellular delivery of GO-203 and thereby targeting of MUC1-C induces anti-cancer activity in vitro and in vivo. These results may also be broadly applicable to the development of other anti-cancer peptides.

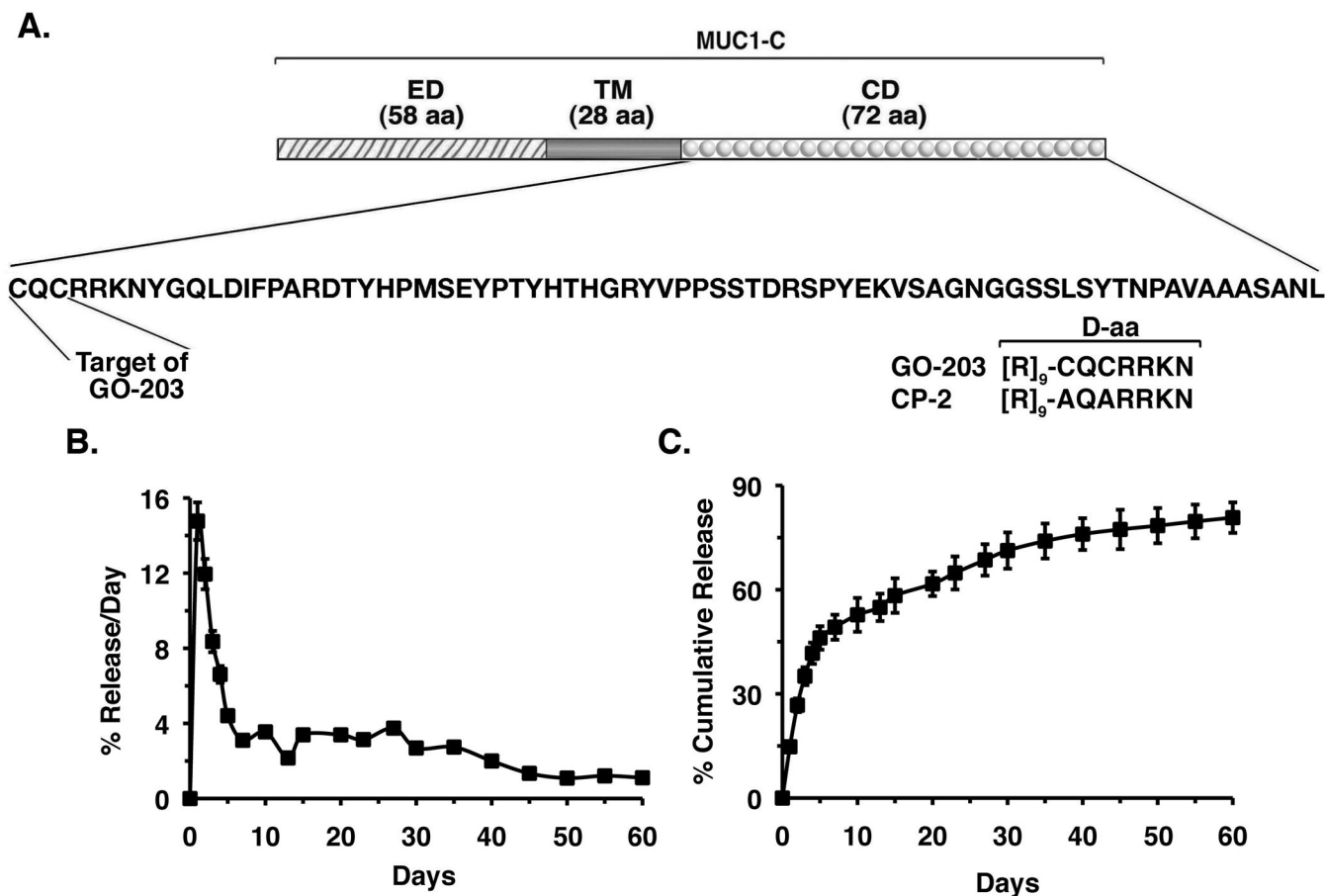
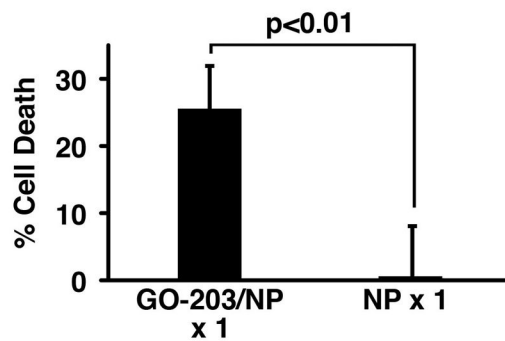
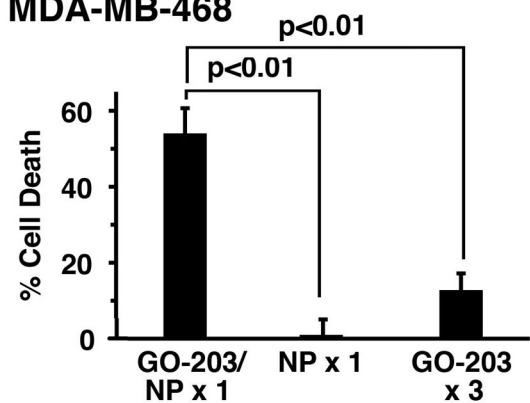
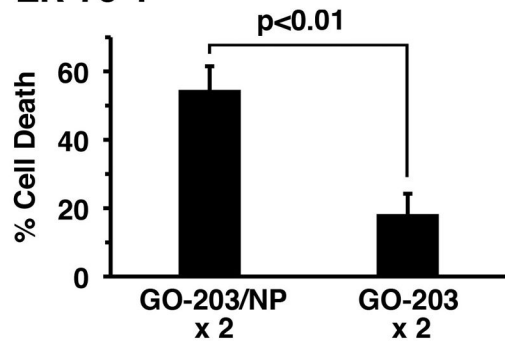
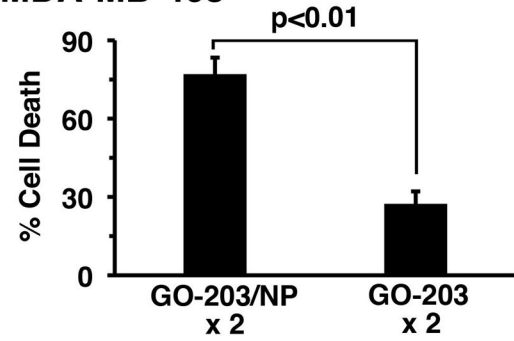
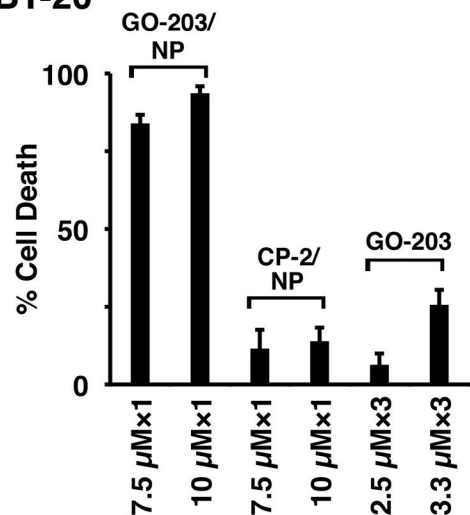
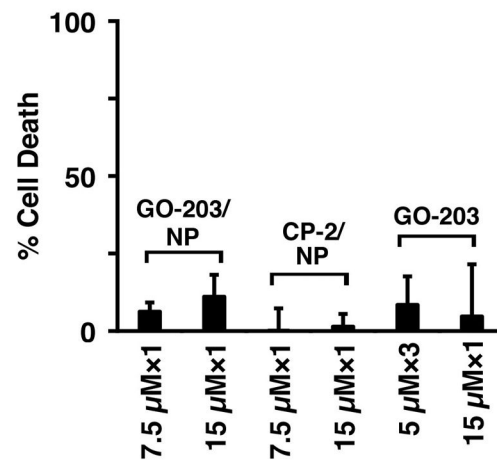


Figure 1. Release of GO-203 from NPs in vitro

A. Schema of the MUC1-C subunit with the 58 aa extracellular domain (ED), 28 aa transmembrane domain (TM) and the 72 aa sequence of the cytoplasmic domain (CD). The CQC motif is necessary for MUC1-C homodimerization and is the target of GO-203 treatment. Also shown are the D-aa sequences of GO-203 and CP-2. B. Release of GO-203 from GO-203/NPs is represented as percent GO-203 released per day (mean \pm SD of three replicates). C. Release of GO-203 from GO-203/NPs represented as percent GO-203 released cumulatively each day (mean \pm SD of three replicates). Additional physical characteristics of the GO-203/NPs are listed in Supplemental Table S2.

A. ZR-75-1**MDA-MB-468****B. ZR-75-1****MDA-MB-468****C. BT-20****D. HCT116****Figure 2. Effects of GO-203/NPs on viability of breast cancer cells**

A. ZR-75-1 cells were treated with 7.5 μM GO-203/NPs or an equal amount of empty NPs once on day 0 (left). The results are expressed as percent cell death (mean±SD of three replicates) as determined by Alamar blue analysis on day 3. MDA-MB-468 cells were treated with 7.5 μM GO-203/NPs or an equal amount of empty NPs once on day 0, or 2.5 μM GO-203 peptide each day for 3 days (right). The results are expressed as percent cell death (mean±SD of three replicates) on day 3. B. ZR-75-1 cells were treated with 2.5 μM GO-203/NPs or 2.5 μM GO-203 on days 0 and 3 (left). The results are expressed as percent

cell death (mean±SD of three replicates) on day 7. MDA-MB-468 cells were treated with 5 μ M GO-203/NPs or 5 μ M GO-203 on days 0 and 3 (right). The results are expressed as percent cell death (mean±SD of three replicates) on day 7. C. BT-20 cells were treated with 7.5 or 10 μ M GO-203/NPs or CP-2/NPs once on day 0. BT-20 cells were also treated with 2.5 or 3.3 μ M GO-203 peptide each day for 3 days. The results are expressed as percent cell death (mean±SD of three replicates) on day 3. D. HCT116 cells were treated with 7.5 or 15 μ M GO-203/NPs or CP-2/NPs once on day 0. HCT116 cells were also treated with 15 μ M GO-203 once on day 0 or 5 μ M GO-203 peptide each day for 3 days. The results are expressed as percent cell death (mean±SD of three replicates) on day 3.

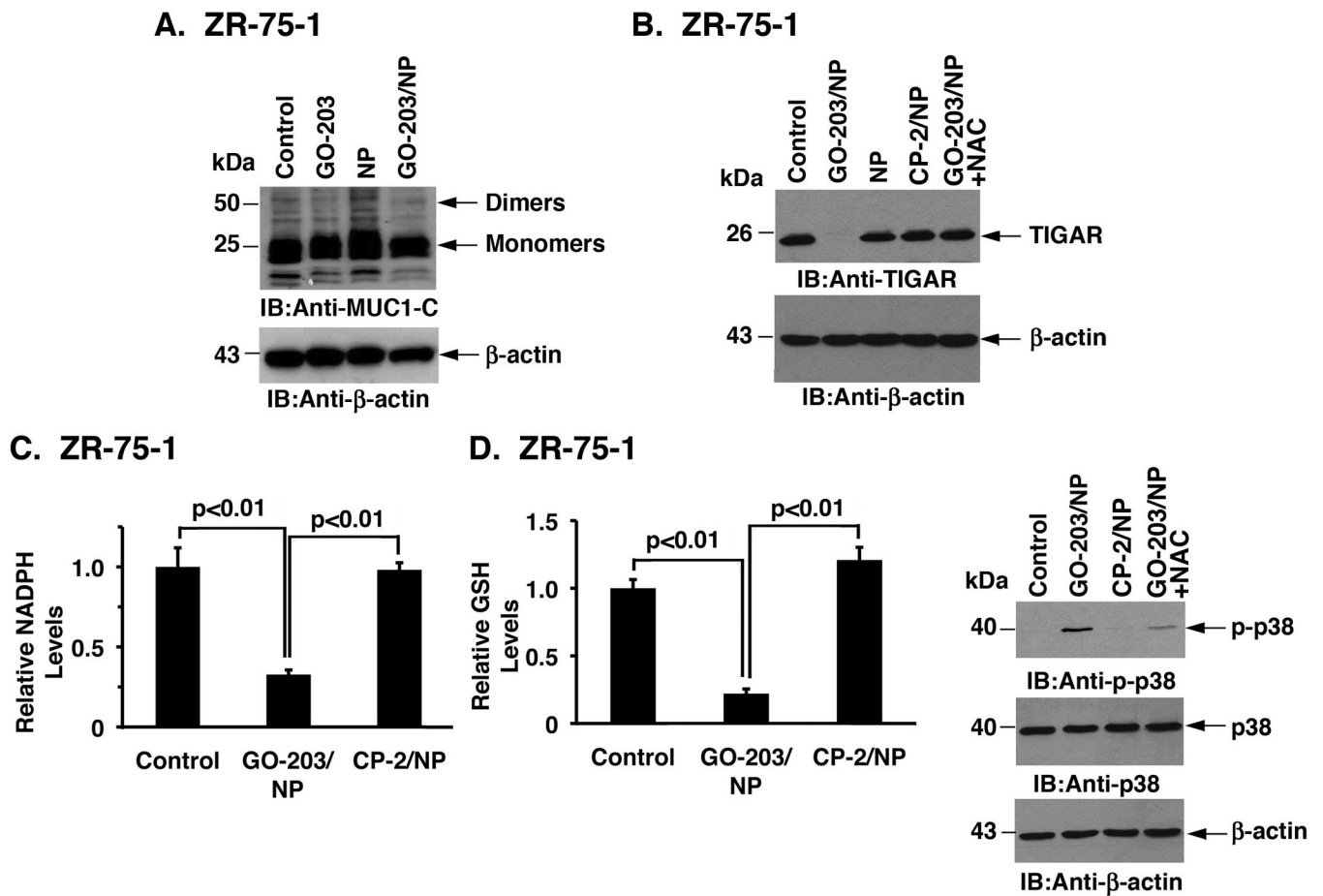


Figure 3. Effects of GO-203/NPs on MUC1-C homodimerization and function in breast cancer cells

A. ZR-75-1 cells were left untreated (Control) or treated with 2.5 μ M GO-203 peptide each day for 3 days. Cells were also treated with 7.5 μ M GO-203/NPs or an equal amount of NPs once on day 0. Whole cell lysates were separated in non-reducing gels and analyzed by immunoblotting with the indicated antibodies. B. ZR-75-1 cells were untreated (Control) or treated with 7.5 μ M GO-203/NPs, 7.5 μ M CP-2/NPs or an equal amount of empty NPs once on day 0 for 2 days. GO-203/NP treated cells were also incubated in the presence of 2.5 mM NAC for 2 days. Lysates were immunoblotted with the indicated antibodies. C. ZR-75-1 cells were left untreated (Control) or treated with 10 μ M GO-203/NPs or CP-2/NPs once on day 0. Cells were analyzed on day 2 for relative NADPH (left) and GSH (right) levels (mean \pm SD of three replicates) as compared to that obtained for the control. D. ZR-75-1 cells were treated with 15 μ M GO-203/NPs or CP-2/NPs for 24 h. GO-203/NP treated cells were also incubated in the presence of 2.5 mM NAC for 24 h. Lysates were immunoblotted with the indicated antibodies.

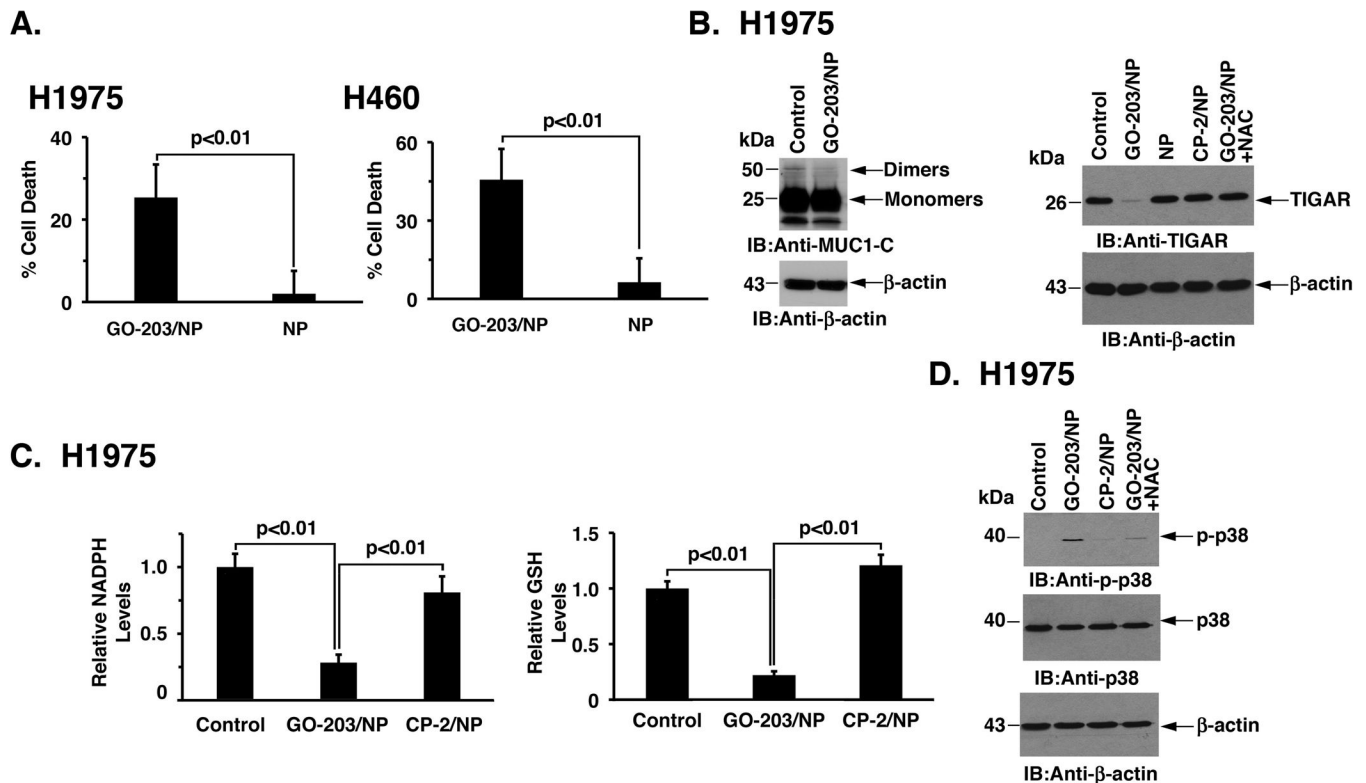


Figure 4. Targeting MUC1-C with GO-203/NPs is effective against NSCLC cells

A. H1975 (left) and H460 (right) cells were treated with 7.5 μ M GO-203/NPs or an equal amount of empty NPs on day 0. The results are expressed as percent cell death (mean \pm SD of three replicates) on day 3. B. H1975 cells were left untreated (Control) or treated with 7.5 μ M GO-203/NPs once on day 0 and cultured for 3 days (left). Whole cell lysates were separated in non-reducing gels and analyzed by immunoblotting with the indicated antibodies. H1975 cells were treated with 7.5 μ M GO-203/NPs, 7.5 μ M CP-2/NPs or an equal amount of empty NPs once on day 0 (right). GO-203/NP treated cells were also incubated in the presence of 2.5 mM NAC. Lysates obtained on day 2 were immunoblotted with the indicated antibodies. C. H1975 cells were left untreated (Control) or treated with 15 μ M GO-203/NPs or CP-2/NPs once on day 0. Cells were analyzed on day 2 for relative NADPH (left) and GSH (right) levels (mean \pm SD of three replicates) as compared to that obtained for the control. D. H1975 cells were left untreated (Control) or treated with 15 μ M GO-203/NPs or CP-2/NPs for 24 h. GO-203/NP treated cells were also incubated in the presence of 2.5 mM NAC for 24 h. Lysates were immunoblotted with the indicated antibodies.

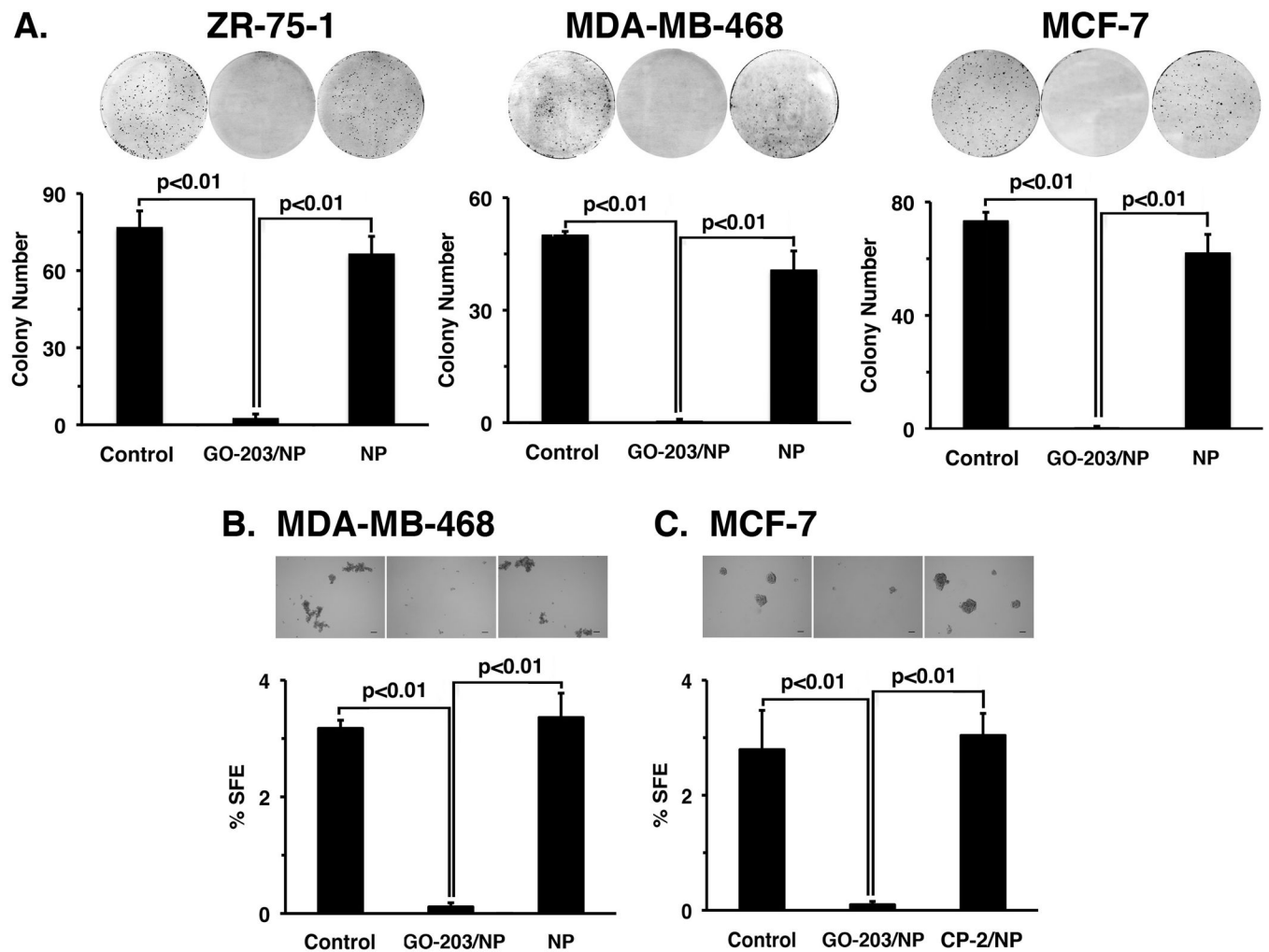


Figure 5. Effects of GO-203/NPs on breast cancer cell self-renewal

A. The indicated breast cancer cells were seeded at 1000 cells/well in 6-well plates and left untreated (Control) or treated with 7.5 μ M GO-203/NPs or an equal amount of empty NPs on day 0. After 3 days, NP containing media was replaced with fresh media. Colonies were stained with crystal violet on day 20 after treatment (upper panels). Colony number (>30 cells) is expressed as the mean \pm SD of three replicates (lower panel). B. MDA-MB-468 cells were left untreated (Control) or treated with 7.5 μ M GO-203/NPs or CP-2/NPs once on day 0. The cells were then plated at 2000 cells/well in sphere culture on day 2. Representative images are shown for the indicated MDA-MB-468 cells grown for 5 days post-treatment in sphere culture (upper panels). Bar represents 100 microns. The percentage SFE is expressed as the mean \pm SD of three determinations (lower panel). C. MCF-7 cells were left untreated (Control) or treated with 7.5 μ M GO-203/NPs or CP-2/NPs once on day 0. The cells were then plated at 2000 cells/well in sphere culture on day 2. Representative images are shown for the indicated MCF-7 cells grown for 5 days post-treatment in sphere culture (upper panels). Bar represents 100 microns. The percentage SFE is expressed as the mean \pm SD of three determinations (lower panel).

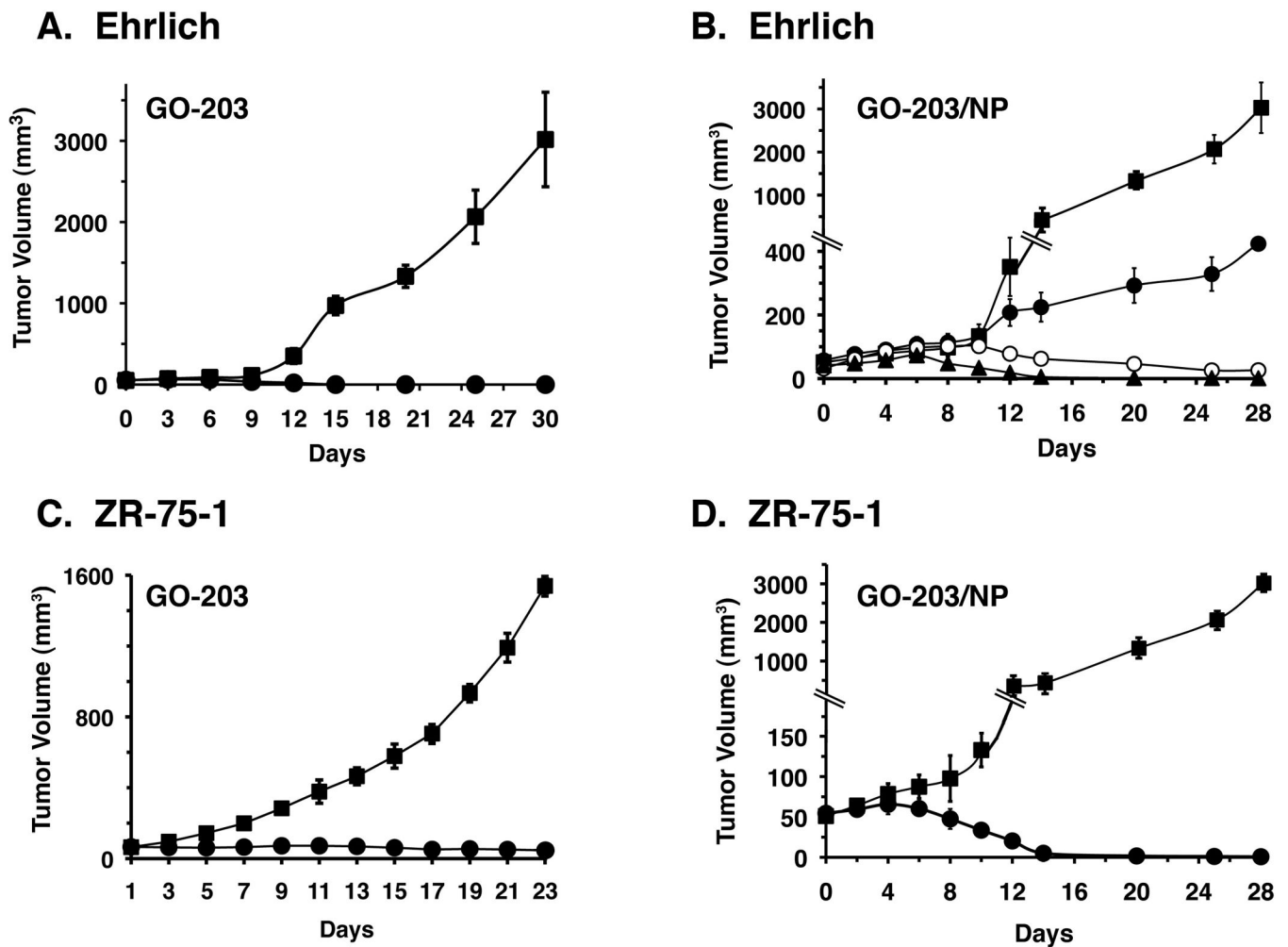


Figure 6. Anti-tumor activity of GO-203/NPs

A and B. Balb/c mice (10 per group) with subcutaneous Ehrlich tumors (~40 mm³) were treated IP with (A) vehicle control (closed squares) or 15 mg/kg GO-203 (closed circles) each day for 21 days, and (B) vehicle control (closed squares), 10 mg/kg (closed circles), 15 mg/kg (open circles) or 20 mg/kg (closed triangles) GO-203/NPs once a week for 3 weeks. Tumor volumes were determined on the indicated days of treatment. The results are expressed as tumor volumes (mean±SEM for 10 mice). C and D. Nude mice (6 per group) with subcutaneous ZR-75-1 tumors (~100 mm³) were treated IP with (C) vehicle control (closed squares) or 18 mg/kg GO-203 each day for 21 days, and (D) vehicle control (closed squares) or 20 mg/kg GO-203/NPs (closed circles) once a week for 3 weeks. Tumor volumes were determined on the indicated days of treatment. The results are expressed as tumor volumes (mean±SEM for 6 mice).